Doppler Shift Estimation for Space-Based AIS Signals Over Satellite-to-Ship Links

JUNFENG WANG[1], **YUE CUI**[2], **HAIXIN SUN**[3], **(Member, IEEE),**
JIANGHUI LI[4], **MINGZHANG ZHOU**[3], **ZEYAD A. H. QASEM**[3],
HAMADA ESMAIEL[5], **(Member, IEEE), AND LANJUN LIU**[6]

[1]School of Electrical and Electronic Engineering, Tianjin University of Technology, Tianjin 300384, China
[2]College of Computer and Information Engineering, Tianjin Normal University, Tianjin 300387, China
[3]School of Information Science and Engineering, Xiamen University, Xiamen 361005, China
[4]Institute of Sound and Vibration Research, University of Southampton, Southampton SO17 1BJ, U.K.
[5]Department of Electrical Engineering, Faculty of Engineering, Aswan University, Aswan 81542, Egypt
[6]College of Engineering, Ocean University of China, Qingdao, 266100, China

Corresponding authors: Junfeng Wang (great_seal@163.com) and Yue Cui (cuiyue_enya@126.com)

ABSTRACT As a communication system for maritime monitoring and navigation, automatic identification system (AIS) has been employed for many years, but its service range is limited in 40 nautical miles. Fortunately, an updated service navigation system named as space-based AIS has been presented in recent years, which can provide global coverage service. However, it encounters the frequency offset issue caused by the relative satellites/ships motion. To cope with it, in this paper, a novel Doppler shift estimation algorithm is proposed for space-based AIS signals over satellite-to-ship wireless fading channels and non-Gaussian noise. In the estimation stage, the signals including the Doppler shift information are first separated from the received ones, but they are also disturbed by the noise. Then, Doppler shift is extracted from the above-detached signals via the higher moments which cancel some excrescent parameters by using several flexible algebra operations, and its estimated expression is presented. Finally, the numerical simulations are carried out to verify the performance of the proposed method, and simulation results demonstrate the benefits of the suggested scheme.

INDEX TERMS Doppler shift, GMSK, Rician fading, space-based AIS, non-Gaussian noise.

I. INTRODUCTION

Automatic identification system (AIS), as an application for short range ship-to-ship and ship-to-coast communications, has emerged as a promising solution to provide maritime surveillance for many water surrounded countries all around the world during the past several years. The AIS was developed to offer various information such as position, identification and speed, initially. Vessels moving on their waters can anticipate and avoid collisions, and coastal guards or search and rescue organizations can detect and track the vessels by these continuous traffic monitoring service information. However, with the increments of ship borne AIS users and

the emerging requirements for some new applications, drawbacks of the AIS, for example, slot collision due to the overload of AIS in very high frequency data link, incommunicable security video information and limited coverage, are becoming increasingly severe. To overcome parts of these questions, a cognitive AIS (CAIS) employing some promising technologies, like spectrum sensing and OFDM, has been proposed in recent years [1]–[4]. Although the CAIS can provide some solutions for the above disadvantages, minimize the maritime traffic accidents and improve the maritime traffic efficiency, it also encounters the serious shortcoming that its radio coverage range is limited in 40 nautical miles. Moreover, with the development of the global commerce, more and more cargoes need to be transported via ships, thus the hazardous or illegal goods may appear. Once it happens, we need to counter and

The associate editor coordinating the review of this manuscript and approving it for publication was Mohammad Tariqul Islam.

improve security by detecting and tracking the ships, but it prevents communications from the ship-to-ship, ship-to-coast, or coast-to-ship equipped the AIS when the distance between vessels or between ships and coast stations is beyond the radio coverage range of the AIS.

Fortunately, satellite communications supply various benefits like wide-band transmission capability, large coverage area, and navigation assistance [5]–[8], which catches significant attention. It is also important for disaster recovery in early period, thanks to ubiquitous coverage over a much larger area (thousands of square kilometers) furnished by the satellites. Based on these excellent merits of the satellite communication, an updated service system termed as the space-based AIS has been suggested in recent years, which provides global coverage range for the maritime traffic observing, illegal transportation monitoring, ocean environment awareness, and so on.

Although the space-based AIS can establish access from the ship-to-ship, ship-to-coast, or coast-to-ship equipped the AIS, it may meet some challenges such as frequency offset cased by relative movement between the space-based AIS and ship borne AIS or terrestrial AIS. To handle the frequency offset, lots of methods have been presented, but they did not consider the multiplicative interference coming from wireless channel fading. Moreover, these contributions are only for additive white Gaussian noise (AWGN). When facing the satellite-to-ship links, the space-based AIS signals will be disturbed by noise coming from the ocean surface that is normally not Gaussian distribution. In order to tackle these issues mentioned above, an algorithm on Doppler shift estimation is proposed in this paper for the space-based AIS signals over the satellite-to-ship wireless channels and non-Gaussian noise. In what follows, we will introduce some features about the space-based AIS, its signal structure, the satellite-to-ship links, and our contributions.

A. SPACE-BASED AIS AND ITS SIGNAL STRUCTURE

The space-based AIS is a new wireless cooperative satellite relaying communication initiative from European space agency and European maritime safety agency, and its purpose in phase B1 is to present the overall system architecture, cost and plan. Although these programmatic ideas look like infant, it paves the way to the space-based AIS project including space and earth segments, especially for space-based AIS signal processing. The space-based AIS information will bring benefit to our maritime activity, but it encounters some technology challenges, such as

- Payload and Message Collision: In the field of view of a satellite, enough reserve is required for information transfer in high traffic zones. Assuming that an LEO satellite serves at an altitude of 650 kilometers, there are around 4000 self-organized time division multiple access (SOTDMA) cells in the line of sight of the spacecraft [8], which results in message collisions at the same time slot and frequency band. Thus, their

FIGURE 1. Burst structure employed by the space-based AIS.

optimization relies on various parameters, for instance, antenna framework, receiver design and appropriate algorithms.

- Signal Strength: Like all satellite communications, the space-based AIS acts as a relaying node situated far from earth. Its received signals are over the up-link channel from the earth and forwarded to the earth. In the space-based AIS, it employs decode and forward protocol (DFP), which uses some methods such as signal separation [9], [10], signal detection [11] and interference cancel [12]. The signal burst format (structure) in the DFP is shown in Fig. 1, which includes 256 bits, and each TDMA frame has 2250 such bursts. It should be noticed that the training sequence and data are both modulated by Gaussian minimum shift keying (GMSK). In the burst format, the transmitter switches on this ramp up slot. The signal strength whichever it is over up-link or down-link is relative weak, due to the long distance between the satellite and the earth, the high path loss and the antenna gain. Accordingly, the weak signal processing is another researched issue.

- Doppler Shift: The relative velocity between the transmitter and the receiver introduces the Doppler shift. For a typical LEO satellite at the altitude of 650 kilometers, the Doppler shift varies around from −4 kHz to 4 kHz according to the relations between the relative velocity and angle, and the carrier frequency. The Doppler shift is beyond the tolerance of the operating frequency for the receiver (3 PPM, i.e., around 486 Hz). In order to tackle this issue, several methods have been presented [13]–[15], but only the AWGN is considered. For the ship-to-satellite or earth-to-satellite up-links, the space-based AIS may not consider multipath fading apart from the free space losses because of the absence of impediments in its link. However, multipath effects are unavoidable besides the line of sight (direct) free space losses over the satellite-to-ship downlinks due to the ocean surface reflections.

The research hots mentioned above are interesting for the academia and industry, but the Doppler shift is the focus in this paper. Moreover, we consider the satellite-to-ship links, which will be introduced in the following subsection.

B. SATELLITE-TO-SHIP LINKS

The maritime satellite communications are relatively mature technology and have been addressed for many years. Like lots of geostationary satellite systems, only three satellites placed above the Pacific, Indian, and Atlantic oceans are able to establish the communication links for all AIS-equipped vessels or coastal stations in almost all navigable ocean areas.

As commented earlier, the communication distances or the service ranges of the AIS are expanded by employing the space-based AIS, but the recovery of signals from the space-based AIS over the satellite-to-ship links has to be done very carefully because of the multipath fading and additive non-Gaussian noise due to signal reflections from the ocean surface, the Doppler shift due to the relative movement between the space-based AIS and the ship borne AIS, and power limitation at the space-based AIS emission, which is also similar to other satellite system designs. In particular, the multipath fading and additive non-Gaussian noise effects can cause a dramatic degradation in bit-error-rate (BER) performance. Therefore, a careful description of the satellite-to-ship links including multiplicative wireless channel interference and additive non-Gaussian noise one is required.

The wireless channels from the satellite to the ship can be characterized by direct and reflected multipath signals from the ocean surface [16]. Actually, an antenna for the ship borne AIS receives multipath signals whichever at the low satellite elevation angles or at the high satellite elevation angles. Several methods have been presented to describe the multipath signals by physical propagation characteristics derived from scattering and reflection effects on rough sea surfaces and antenna properties, whose corresponding models usually are complex and contain useful parameters to analyze the influence on the data transmission. If the multipath signal comes from the reflections of many statistical independent points on the surface, the multiplicative distortion signals can be modelled as statistically independent Gaussian random processes. Moreover, the experiments demonstrate that no significant specular reflections have been found except for the calm sea surface that would cause a discrete specular signal, which seems that this assumption about diffuse reflections is reasonable [16]. The experiment also indicates that the Rician model for the fading process is appropriate. When the maximum time difference of the multipath signals is significantly less than the reciprocal of bandwidth, a time varying non-frequency selective fading channel is reasonable. In addition, for applications using a communication channel bandwidth of maximal 25-50 kHz, the channel of the maritime satellite communications may be considered as the non-frequency selective fading [16]. Thus, as a channel bandwidth of 25 kHz for the space-based AIS, the wireless channels from the satellite to the ship can be regarded as a non-frequency selective Rician fading process.

It is well known that there are some influences of the additive noise on the systemic performance besides the multiplicative wireless channels. Generally, the additive noise in most scenarios is assumed as Gaussian distribution, which is not because of its fitness to noise data but because of its mathematical tractability. Moreover, the most of theoretical analyses have been carried out, which is based on the assumption of the Gaussian distribution. However, from the experimental measurements, it is evident that the additive noises over the sea surface ambiance are non-Gaussian [17]–[19]. In practice, the non-Gaussian process with heavy tails can occur in many different forms, one of which is Gaussian mixture model (GMM). The GMM can describe a heavy-tailed distribution well that has greater tail probabilities than one suggested by the Gaussian model, which is used in this paper to model the additive noise.

C. CONTRIBUTIONS AND ORGANIZATIONS

This paper addresses the problem of the Doppler shift estimation, which is for the space-based AIS signals over the satellite-to-ship links. In the estimation procedure, the benefits of the proposed algorithm are:

1) The proposed method can handle the multiplicative non-frequency selective Rician fading channel interference, which employs statistical characteristics of the Rician fading channels.
2) The proposed method can deal with the additive non-Gaussian noise interference that can be generated by the GMM. The GMM can represent various classes of continuous functions with reasonable accuracy, whose statistical properties are also utilized in this paper.
3) The proposed method can cancel some nuisance parameters by mathematical operations, which avoids error propagation due to extra parameter estimation in the model.
4) The proposed method is robust with respect to the estimated frequency in its range with the Rice factor increments and all kinds of the non-Gaussian noise generated by the GMM model, which is verified by computer simulations.

In the following, we give the organizations of this paper. Section II explains the background with respect to received signal model, for instance, GMSK modulation signal, the non-frequency selective Rician fading channels and the GMM, and states the problem. Section III presents Doppler shift estimation algorithm for space-based AIS signals over the satellite-to-ship links in detail. The proposed method in this work is verified by computer simulations in Section IV, and the conclusion part in Section V summarizes the results and discusses possible applications of the presented approach.

II. PRELIMINARY AND PROBLEM FORMULATION

In this section, the received signal model is first described. Then, we present some background materials on the signal model, including the GMSK modulation signal, the fading channels, the GMM, and problem which will be solved in the sequel.

A. RECEIVED SIGNAL MODEL AND ITS BACKGROUND

The baseband received signals over the satellite-to-ship links can be expressed as

$$y(t) = x(t) \cdot h(t) + w(t), \qquad (1)$$

where $x(t)$ is the GMSK modulation signal, $h(t)$ is the non-frequency selective Rician fading channel coefficient, and $w(t)$ is the non-Gaussian noise.

$$p(t) = \int_{-\infty}^{t} g(\tau) \, d\tau = \frac{1}{2} \int_{-\infty}^{t} \left\{ erfc \left[\frac{2\pi B}{\sqrt{2ln2}} \left(\tau - \frac{T_b}{2} \right) \right] - erfc \left[\frac{2\pi B}{\sqrt{2ln2}} \left(\tau + \frac{T_b}{2} \right) \right] \right\} d\tau, \tag{4}$$

From the introduction mentioned above, the (forwarded) signal transmitted by the space-based AIS is modulated by the GMSK. A brief review of the GMSK modulation signal, $x(t)$, is presented as

$$x(t) = exp(j \cdot \Theta(a_i, t)), \tag{2}$$

where,

$$\Theta(a_i, t) = \pi \sum_i a_i \cdot p(t - iT_b), \tag{3}$$

here a_i is information sequence, T_b is symbol period, and $p(\cdot)$ is phase pulse response and denoted by (4) at the top of this page, in which $g(\cdot)$ is the rectangular impulse response of Gaussian filter, B is 3 dB bandwidth of this Gaussian filter, and $erfc(\cdot)$ is given by

$$erfc(t) = \frac{2}{\sqrt{\pi}} \int_t^{\infty} exp(-\tau^2) \, d\tau \tag{5}$$

Theoretically speaking, the rectangular impulse response of Gaussian filter is infinite. For its physical realization, it can be truncated into L bits. Thus, with respect to (3), when $nT_b \leq t \leq (n+1)T_b$, it can be written as

$$\Theta(a_i, t) = \pi \sum_{i=n-(L+1)/2+1}^{n+(L-1)/2} a_i \cdot p(t - iT_b) + \frac{\pi}{2} \sum_{i=1}^{n-(L+1)/2} a_i, \tag{6}$$

where,

$$p(t) = \begin{cases} 0, & t < -\frac{(L-1)T_b}{2} \\ \frac{1}{2T_b} \int_{-\infty}^{t} g(\tau - \frac{T_b}{2}) \, d\tau, & -\frac{(L-1)T_b}{2} \leq t \leq \frac{(L+1)T_b}{2} \\ \frac{1}{2}, & t > \frac{(L+1)T_b}{2} \end{cases} \tag{7}$$

To date, the non-frequency selective Rician fading channel mentioned in this paper, $h(t)$, has been simulated and modelled in most of works, see [20], [21] and the references therein, which can be described as

$$h(t) = \sqrt{\frac{K}{1+K}} h_{LoS}(t) + \sqrt{\frac{1}{1+K}} h_{NLoS}(t), \tag{8}$$

where K is Rice factor, $h_{NLoS}(t)$ is non-frequency selective Rayleigh non line of sight (NLoS) fading component, whose mean and autocorrelation function are zero and zero-order Bessel function, respectively, and whose real and imaginary parts are independent Gaussian random variables that can be modeled by various schemes detailedly addressed in [20], and $h_{LoS}(t) = exp(j2\pi f_d t cos\theta_0 + j\phi_0)$ is line of sight (LoS) component with f_d, θ_0, and ϕ_0 being the maximum Doppler shift, angle of arrival, and initial phase, respectively.

From (8), we can also see that the Doppler shift is what we want to estimate.

From the foregoing, the non-Gaussian noise can be generated by the GMM which is the weighted sum of multiple Gaussian components, and we assume that the non-Gaussian noise is with zero-mean for sake of simplicity, namely, its distribution (probability density function, PDF) is

$$f(w) = \sum_i \epsilon_i \cdot \mathcal{CN}(w|\mu_i = 0, \sigma_i), \tag{9}$$

where $\mathcal{CN}(\cdot)$ is complex Gaussian PDF, $\mu_i = 0$, σ_i and ϵ_i are zero-mean, standard deviation and weight (probability) of the ith Gaussian component, respectively. Here, the term ϵ_i satisfies $\sum_i \epsilon_i = 1$. According to above distribution, the total non-Gaussian noise variance is given by $\sigma_w^2 = \sum_i \epsilon_i \cdot \sigma_i^2$.

B. PROBLEM STATEMENTS

Throughout the above background, one can notice that the estimated Doppler shift is concealed in the non-frequency selective Rician fading channels, but its extraction does not seem as easy as being able to want. To examine the estimated method of the Doppler shift, at the beginning, we discretize (1) and rewrite it as

$$y(n) = x(n) \cdot h(n) + w(n) \tag{10}$$

Intuitively, it should discard some of trashy signals and excrescent parameters such as the GMSK modulation signals, the Rice factor, the initial phase of the LoS component, the NLoS component, and the non-Gaussian noise signal, if one wants to extract the Doppler shift from the received signal model correctly. Via the above characterization, if we do not consider the non-Gaussian noise signal, a kind of method named as data aided parameter estimated one is employed by utilizing the training sequence to cancel the GMSK modulation signal. Thus, we do a simulation about $y'(n) = x(n) \cdot h(n)$ with $y'(n) \cdot x^*(n)$, here $x^*(\cdot)$ denotes conjugation of the $x(\cdot)$. The simulation results are shown in Fig. 2, where $BT_b = 0.4$, $L = 3$, a_i is the "-1 $-$ 1 1 1 -1 -1 1 1 -1 -1 1 1 -1 $-$ 1 1 1 -1 -1 1 1 -1 -1 1 1" which is the training sequence, and sampling rate is $8/T_b$. As can be seen in the figure, $h(n)$ enveloping the estimated Doppler shift is recovered without any loss in quality, although $x(n)$ seems very complex. The above results abridge the distance of our aim, but it is disturbed by the non-Gaussian noise. Generally, the non-Gaussian noise is regarded as independent and identically distributed (i.i.d.) one and widely adopted in many literatures. In other words, $E\{w(n)w^*(n-m)\} = \sigma_w^2 \delta(m)$, $\forall m$, and $f(w(n)) = f(w(m))$, $\forall n \neq m$, where $E\{\cdot\}$ is the statistical average operator, and $\delta(\cdot)$ is the Kronecker delta function. Here, we do another simulation experiment about
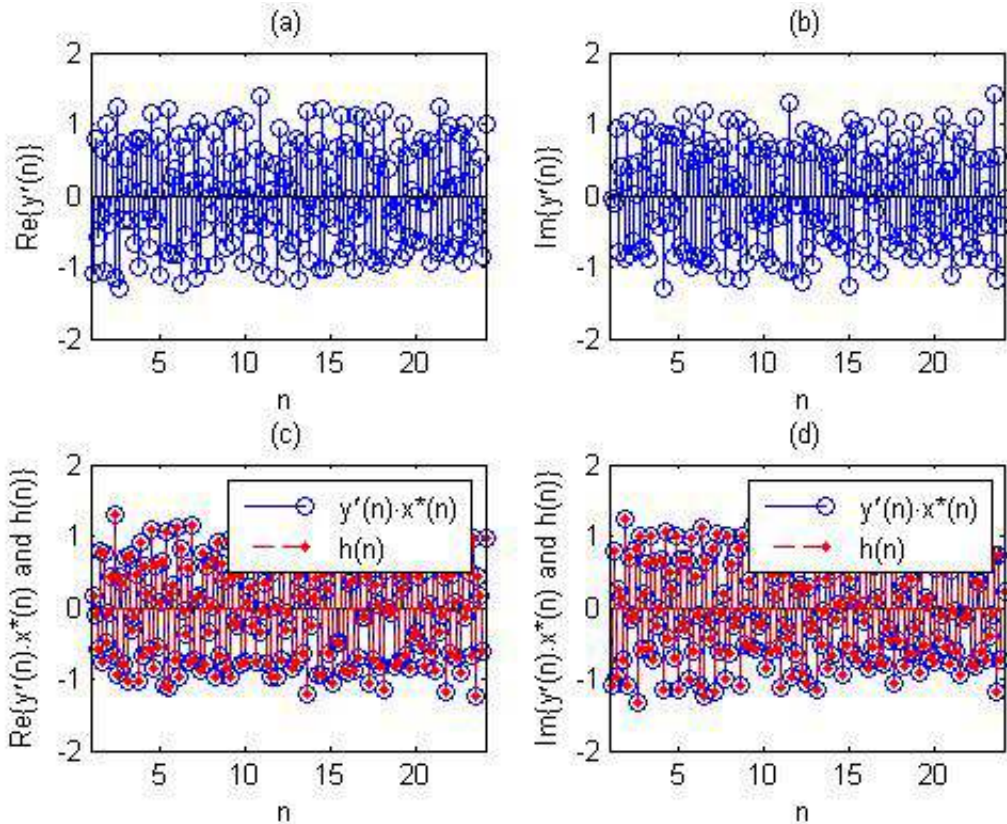
FIGURE 2. A simple simulation about extraction of the $h(n)$ enveloping the estimated Doppler shift: (a) and (b) are the real and imaginary parts of the $y'(n)$, respectively; (c) and (d) are the real and imaginary parts of the $y'(n) \cdot x^*(n)$ and $h(n)$, respectively.
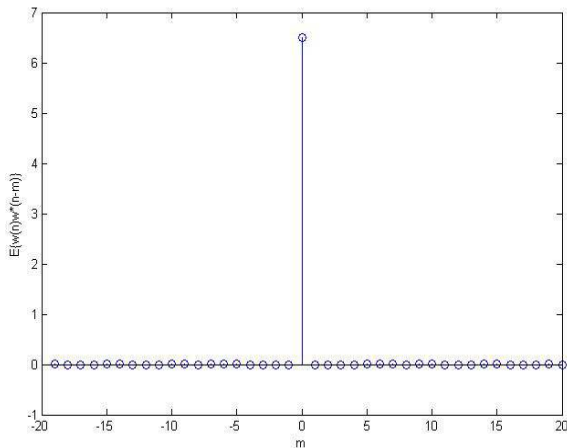

FIGURE 3. A simulation result about the $E\{w(n)w^*(n-m)\}$.

$E\{w(n)w^*(n-m)\}$ as shown in Fig. 3. Furthermore, it should be mentioned that the results in this simulation for $|m| > 0$ and $n \ll \infty$ (or not large enough) are the absolute values of correlation function, which also demonstrates that the non-Gaussian noise $w(n)$ is statistically independent.

It can be seen from the above experiments that the data aided method and the i.i.d. statistical characterization of the noise are motive for the proposed algorithm. In the

succeeding section, we discuss the challenges involved in the estimation of the Doppler shift about the space-based AIS signals over the non-frequency selective Rician fading channels and the non-Gaussian noise, and their solutions.

III. CHALLENGES AND PROPOSED ALGORITHM

As can be seen from the previous discussion, it is very difficult to extract the Doppler shift from (10) directly, because of the unnecessary parameters such as the Rice factor, the initial phase of the LoS component, and the NLoS component except for the non-Gaussian noise and the GMSK modulation signal. Although it is not an easy task, we can cancel the effect of the GMSK modulation signal by multiplying (10) and $x^*(n)$ together from the preceding detailed discussion, i.e.,

$$z(n) = y(n) \cdot x^*(n) = h(n) + v(n), \qquad (11)$$

where $v(n) = w(n) \cdot x^*(n)$ is also the non-Gaussian noise with zero-mean.

From (11), we can clearly see that the GMSK modulation signal has been dropped out, but the extraction of the $h(n)$ enveloping the estimated Doppler shift needs to eliminate the non-Gaussian noise, and the influence of the non-Gaussian noise on the extraction of the Doppler shift can be illustrated in Fig. 4. Therefore, in this section, we then consider the
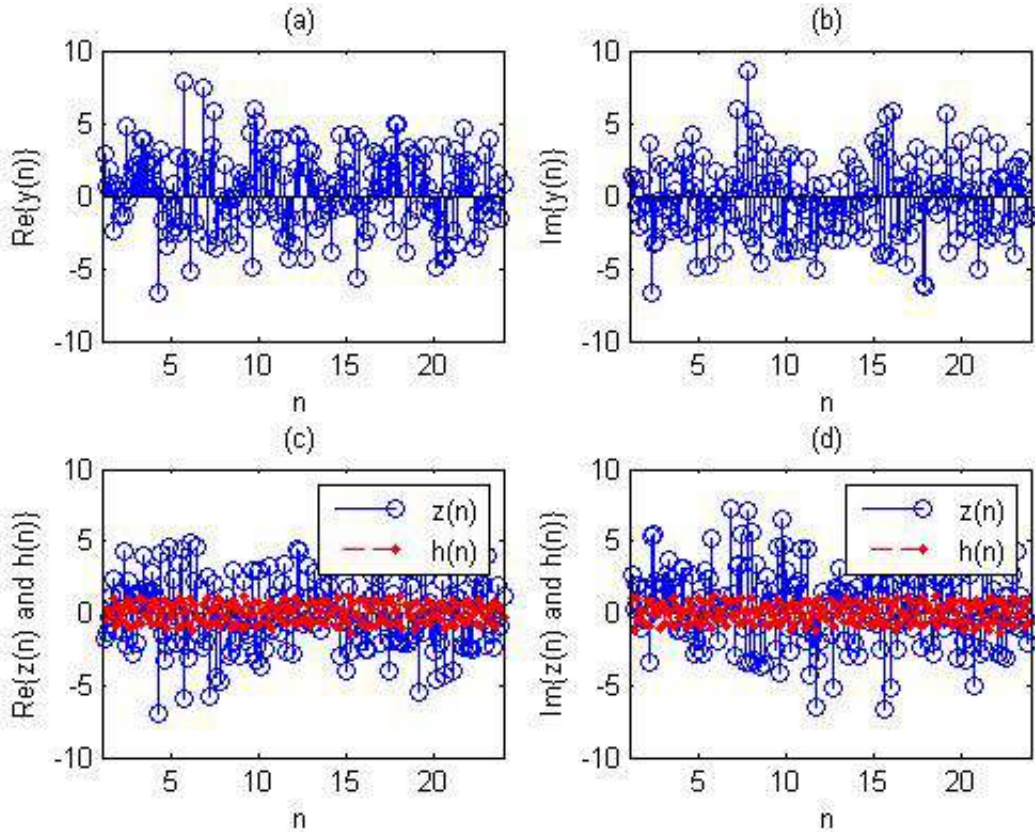
FIGURE 4. A simulation experiment about the influence of the non-Gaussian noise on the extraction of the Doppler shift: (a) and (b) are the real and imaginary parts of the $y(n)$, respectively; (c) and (d) are the real and imaginary parts of the $z(n)$ and $h(n)$, respectively.

second-order moment (autocorrelation) to remove the effects of the non-Gaussian noise, i.e., it is defined as

$$R_{zz}(m) \triangleq E\{z^*(n) \cdot z(n+m)\} \quad (12)$$

After substituting (11) into (12) and doing some algebra operations, it can be written as

$$R_{zz}(m) = \frac{K}{1+K} exp\left(j2\pi \Delta f_d m\right) + \frac{1}{1+K} J_0\left(2\pi f_d m\right) + \sigma_v^2 \delta(m), \quad (13)$$

where $\Delta f_d = f_d \cos \theta_0$ is the Doppler shift to be estimated, $J_0(\cdot)$ is the zero-order Bessel function, the mean of the non-Gaussian noise $v(\cdot)$ is assumed as 0 as mentioned above, and σ_v^2 is the variance of the non-Gaussian noise. During the computation of the (13), $E\{v(n)\} \equiv 0$, $E\{v^*(n)\} \equiv 0$, $E\{v^*(n)v(n+m)\} \equiv \sigma_v^2 \delta(m)$, $E\{h_{NLoS}(n)\} \equiv 0$, $E\{h_{NLoS}^*(n)\} \equiv 0$, and $E\{h_{NLoS}^*(n)h_{NLoS}(n+m)\} \equiv J_0\left(2\pi f_d m\right)$ are utilized. Please see Appendix A for detailed derivation.

From (13), we also see that the Doppler shift is unfeasible to be estimated directly due to the K and the $J_0(\cdot)$. In order to remove these parameters and function, we give the fourth-order moment which is defined as

$$R_{zzzz}(l, m, q) \triangleq E\{z^*(n) \cdot z(n+l) \cdot z(n+m) \cdot z^*(n+q)\} \quad (14)$$

Substituting (11) into (14) and doing some algebra operations, we obtain

$$R_{zzzz}(l, m, q) = \left(\frac{K}{1+K}\right)^2 exp\left(j2\pi \Delta f_d(l + m - q)\right)$$

$$+ \frac{K}{1+K} exp\left(j2\pi \Delta f_d l\right) \sigma_v^2 \delta(m - q)$$

$$+ \frac{K}{(1+K)^2} exp\left(j2\pi \Delta f_d l\right) J_0\left(2\pi f_d(m - q)\right)$$

$$+ \frac{K}{(1+K)^2} exp\left(j2\pi \Delta f_d m\right) J_0\left(2\pi f_d(l - q)\right)$$

$$+ \frac{K}{1+K} exp\left(j2\pi \Delta f_d m\right) \sigma_v^2 \delta(l - q)$$

$$+ \frac{1}{1+K} J_0\left(2\pi f_d m\right) \sigma_v^2 \delta(l - q)$$

$$+ \frac{K}{(1+K)^2} exp\left(j2\pi \Delta f_d(l - q)\right) J_0\left(2\pi f_d m\right)$$

$$+ \frac{K}{(1+K)^2} exp\left(j2\pi \Delta f_d(m - q)\right) J_0\left(2\pi f_d l\right)$$

$$+ \frac{1}{1+K} J_0\left(2\pi f_d l\right) \sigma_v^2 \delta(m - q)$$

$$+ \frac{K}{1+K} exp\left(j2\pi \Delta f_d(l - q)\right) \sigma_v^2 \delta(m)$$

$$+ \frac{1}{1+K} J_0\big(2\pi f_d(l-q)\big)\sigma_v^2\delta(m)$$

$$+ \frac{K}{1+K} exp\big(j2\pi \, \Delta f_d(m-q)\big)\sigma_v^2\delta(l)$$

$$+ \frac{1}{1+K} J_0\big(2\pi f_d(m-q)\big)\sigma_v^2\delta(l)$$

$$+ \frac{1}{(1+K)^2}\Big\{ J_0\left(2\pi f_d l\right) J_0\big(2\pi f_d(m-q)\big)$$

$$+ J_0\left(2\pi f_d m\right) J_0\big(2\pi f_d(l-q)\big)\Big\}$$

$$+ \sigma_v^4\delta(l)\delta(m-q) + \sigma_v^4\delta(m)\delta(l-q), \quad (15)$$

here, besides the identity used by (13), in the process of calculating (15), $E\{(h_{NLoS}(n+l)h_{NLoS}(n+m))^*\} \equiv 0$, $E\{h_{NLoS}(n+m)h_{NLoS}(n+l)\} \equiv 0$, $E\{h_{NLoS}^*(n)h_{NLoS}(n+m)h_{NLoS}(n+l)\} \equiv 0$, $E\{h_{NLoS}(n+l)h_{NLoS}(n+m)h_{NLoS}^*(n+q)\} \equiv 0$, $E\{h_{NLoS}^*(n)h_{NLoS}(n+m)h_{NLoS}^*(n+q)\} \equiv 0$, $E\{h_{NLoS}^*(n)h_{NLoS}(n+l)h_{NLoS}^*(n+q)\} \equiv 0$, $E\{h_{NLoS}^*(n)h_{NLoS}(n+l)h_{NLoS}(n+m)h_{NLoS}^*(n+q)\} \equiv E\{h_{NLoS}^*(n)h_{NLoS}(n+l)\} E\{h_{NLoS}(n+m)h_{NLoS}^*(n+q)\} + E\{h_{NLoS}^*(n)h_{NLoS}(n+m)\} E\{h_{NLoS}(n+l)h_{NLoS}^*(n+q)\}$, $E\{(v(n+m)v(n+l))^*\} \equiv 0$, $E\{v(n+m)v(n+l)\} \equiv 0$, $E\{v^*(n)v(n+m)v(n+l)\} \equiv 0$, $E\{v(n+l)v(n+m)v^*(n+q)\} \equiv 0$, $E\{v^*(n)v(n+m)v^*(n+q)\} \equiv 0$, $E\{v^*(n)v(n+l)v^*(n+q)\} \equiv 0$, and $E\{v^*(n)v(n+l)v(n+m)v^*(n+q)\} \equiv E\{v^*(n)v(n+l)\}E\{v(n+m)v^*(n+q)\}+E\{v^*(n)v(n+m)\}E\{v(n+l)v^*(n+q)\}$ are employed. See Appendix B for detailed derivation.

It is obvious from (13) and (15) that the Rice factor and Bessel function similarly include in both equations. Therefore, we can do some mathematical operations on the (13) and (15) to estimate the Doppler shift Δf_d. We set $m = 0, l = 0$ and $q = 0$, substitute (13) into (15), and get

$$R_{zzzz}(0, 0, 0) = -\left(\frac{K}{1+K}\right)^2 + 2R_{zz}^2(0) \quad (16)$$

From the above equation, it is clearly seen that the Rice factor K can be solved. In what follows, we dispel the Bessel function $J_0(\cdot)$ in the (13) and (15), simultaneously. Thus, by setting $m \neq 0$ and substituting (13) into (15) with $l = 0$ and $q = 0$, we obtain

$$R_{zzzz}(0, m, 0) = -\left(\frac{K}{1+K}\right)^2 exp(j2\pi \, \Delta f_d m)$$
$$+ 2R_{zz}(m)R_{zz}(0) \quad (17)$$

Then, we substitute (16) into (17) and do some simple algebra operations, and it can be written as

$$\widehat{\Delta f_d} = \frac{1}{2\pi m} \cdot arg\left\{\frac{R_{zzzz}(0, m, 0) - 2R_{zz}(m)R_{zz}(0)}{R_{zzzz}(0, 0, 0) - 2R_{zz}^2(0)}\right\}, \quad (18)$$

where $arg\{\cdot\}$ stands for phase extracting operation, and let $\Phi(m) = arg\left\{\frac{R_{zzzz}(0,m,0)-2R_{zz}(m)R_{zz}(0)}{R_{zzzz}(0,0,0)-2R_{zz}^2(0)}\right\}$.

Theoretically speaking, the above equation is only an estimation of the Doppler shift Δf_d for a given m. Therefore, we can employ the phase difference, i.e., $\Phi(m) - \Phi(m-1)$,

$\forall m$, to improve accuracy of the estimation. Based on the analyses, discussions, and mathematical derivation mentioned above, we conclude the algorithm proposed in this paper for the Doppler shift estimation on space-based AIS signals over satellite-to-ship links in Algorithm 1.

Algorithm 1 Doppler Shift Estimation on Space-Based AIS Signals Over Satellite-to-Ship Links

---

Input: $y(n)$
Output: $\widehat{\Delta f_d}$
1: Get $z(n)$ as in (11)
2: **for** $m = 2$ to the setting maximum value of the m **do**
3:    Calculate $\varphi(m) = \Phi(m) - \Phi(m-1)$ based on (13) and (15)
4:    Calculate $\widehat{\Delta f_d}(m) = \frac{1}{2\pi}\varphi(m)$
5: **end for**
6: **return** $\widehat{\Delta f_d}$ on the averaging of $\widehat{\Delta f_d}(m)$

The challenges and their solutions, i.e., the proposed algorithm on the Doppler shift estimation for the space-based AIS signals over the satellite-to-ship links, clearly describe the mechanism of the estimation on Doppler frequency. Generally speaking, except for the simple mathematical form of the estimated components, we further need to understand performance of the proposed method. Thus, in the following, we will provide a detail evaluations on the suggested algorithm for several conditions of interest via computer simulation.

IV. NUMERICAL RESULTS AND DISCUSSIONS

In this section, a received space-based AIS signal over the satellite-to-ship links including the non-frequency selective Rician fading channels and non-Gaussian noise is considered for simulation and analysis. The non-frequency selective Rician fading channels are generated by [20], and the non-Gaussian noise with $\mu = 0$ is produced by the GMM with various parameters σ_i and ϵ_i for different scenarios in all numerical results. The simulation results are obtained by averaging over 50,000 Monte Carlo trials. The carrier frequency, BT_b and L are set as 161.975 MHz, 0.4 and 3, respectively. The sampling rate is set as $32/T_b$. The training sequence is employed in the estimation procedure, and Doppler shift is assumed as a constant value in one burst duration unless otherwise specified.

A. $\widehat{\Delta F_D}$ AND ΔF_D VS. θ_0

In this subsection, the estimated Doppler shift ($\widehat{\Delta f_d}$) and theoretical one (Δf_d) versus the angle of arrival (θ_0) from 0 to π are shown in Fig. 5 for the maximum Doppler shift $f_d = 5$, 4, and 3 kHz, where parameters of the non-Gaussian noise are set as $i = 1, 2, 3$, $\sigma_1^2 = 0.05$, $\sigma_2^2 = 0.01$, $\sigma_3^2 = 0.63$, $\epsilon_1 = 0.51$, $\epsilon_2 = 0.31$, and $\epsilon_3 = 0.18$, signal-to-noise ratio (SNR) is set as 30 dB, and the Rice factor (K) is set as 15. From this simulation experiment, it verifies the effect of the θ_0 variations on the Doppler shift. Further, it is also
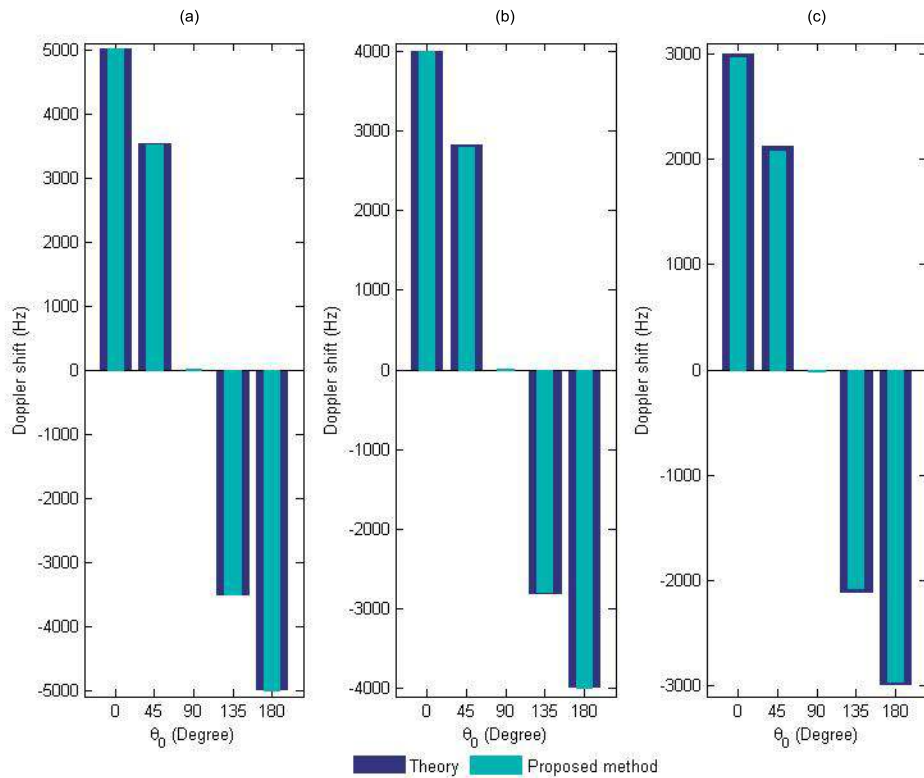
FIGURE 5. The estimated Doppler shift ($\widehat{\Delta f_d}$) and theoretical one (Δf_d) versus the θ_0 for (a) the maximum Doppler shift $f_d = 5$ kHz, (b) $f_d = 4$ kHz, and (c) $f_d = 3$ kHz, respectively.

seen that the proposed scheme works close to the ideal one. That is to say, the estimated Doppler shift is almost unbiased, i.e., $\widehat{\Delta f_d} \doteq \Delta f_d$, which indicates that the proposed method can provide the good estimated results.

B. STD OF $\widehat{\Delta F_D}$ VS. SNR

In the following subsections, the standard deviation (STD) of the estimated Doppler shift ($\widehat{\Delta f_d}$) is chosen as the performance index to further evaluate our proposed algorithm. Furthermore, the estimated method based on the (13) is presented to compare with our suggested scheme. The STD of the $\widehat{\Delta f_d}$ versus the SNR is illustrated in Fig. 6, where some parameters are the same as the first subsection except for the SNR and Rice factor. The K is set as 10, and the SNR varies from 2 to 30 dB. As seen from these results, the STDs are approximately 15 Hz and 45 Hz for the proposed algorithm and the method based on the (13) at the f_d mentioned in this subsection, respectively. Compared with the method based on the (13), our proposed method can provide the better estimation on the Doppler shift. Moreover, from the above results, we also conclude that the STD of the estimated Doppler shift ($\widehat{\Delta f_d}$) of our proposed scheme is robust to the SNR above 0 dB for various f_d, but the STD on the method based on the (13) has a small vibration due to the influence of the Rice factor and the Bessel function of the first and second items on the right side of the (13). Further speaking, our proposed algorithm is robust to the
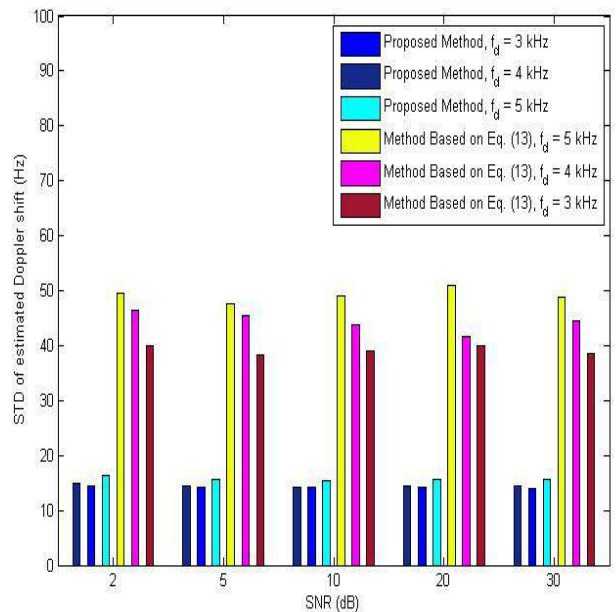

FIGURE 6. The STD of the estimated Doppler shift ($\widehat{\Delta f_d}$) versus the SNR.

SNR above 0 dB for various scenarios on the maximum Doppler shift.

C. STD OF $\widehat{\Delta F_D}$ VS. K

In this subsection, we evaluate the influence of the Rice factor on the estimation performance of the Doppler shift in Fig. 7.
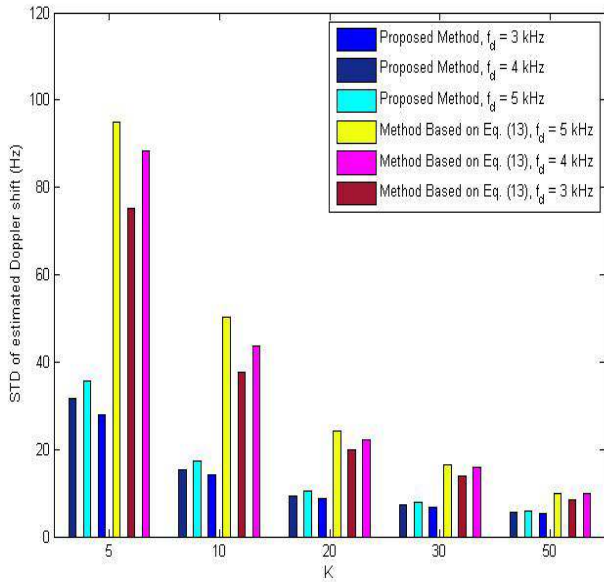
FIGURE 7. The STD of the estimated Doppler shift ($\widehat{\Delta f_d}$) versus the *K*.

FIGURE 8. The STD of the estimated Doppler shift ($\widehat{\Delta f_d}$) versus the non-Gaussian noise for different parameters (σ_i and ϵ_i).

The parameters of the non-Gaussian noise and maximum Doppler shift are the same as the above scenarios. The SNR is set as 20 dB, and the *K* varies from 5 to 30. It can be noticed from the figure that the estimated accuracy becomes much better when the Rice factor increases. Actually, these results indicate that the effect of Rayleigh component on the main component (LoS) is less as the Rice factor increases. In other words, the scatter components propagated via differently indistinguishable NLoS paths are significantly weak. Compared with Fig. 6, the effect of the Rice factor on performance appears to dominate. Further, as predicted, the performance of our investigated algorithm surpasses that of the method based on the (13) under small *K*, and they both can be improved with the Rice factor increments.

D. STD OF $\widehat{\Delta F_D}$ VS. σ_I AND ϵ_I

In this subsection, the effect of the non-Gaussian noise with different parameters on the estimation performance of the Doppler shift is investigated in Fig. 8. The SNR is set as 20 dB, and the *K* is set as 20. We also consider the three sets of different parameters for the non-Gaussian noise: herein, we set $i = 1, 2, 3$, v_1: $\sigma_1^2 = 0.05$, $\sigma_2^2 = 0.01$, $\sigma_3^2 = 0.63$, $\epsilon_1 = 0.51$, $\epsilon_2 = 0.31$, and $\epsilon_3 = 0.18$; v_2: $\sigma_1^2 = 0.02$, $\sigma_2^2 = 0.06$, $\sigma_3^2 = 0.88$, $\epsilon_1 = 0.21$, $\epsilon_2 = 0.51$, and $\epsilon_3 = 0.28$; and v_3: $\sigma_1^2 = 0.01$, $\sigma_2^2 = 0.16$, $\sigma_3^2 = 1.48$, $\epsilon_1 = 0.31$, $\epsilon_2 = 0.21$, and $\epsilon_3 = 0.48$. It can be seen from Fig. 8 that there are 3 pieces of the data on the non-Gaussian noise with different PDF, and the probabilities of the tail are much greater among these 3 scenarios. Importantly, it can be noticed from the figure that the STDs of the estimated Doppler shift are almost same for all scenarios mentioned above. Thus, we also conclude that the proposed scheme and the method based on the (13) are both robust with respect to
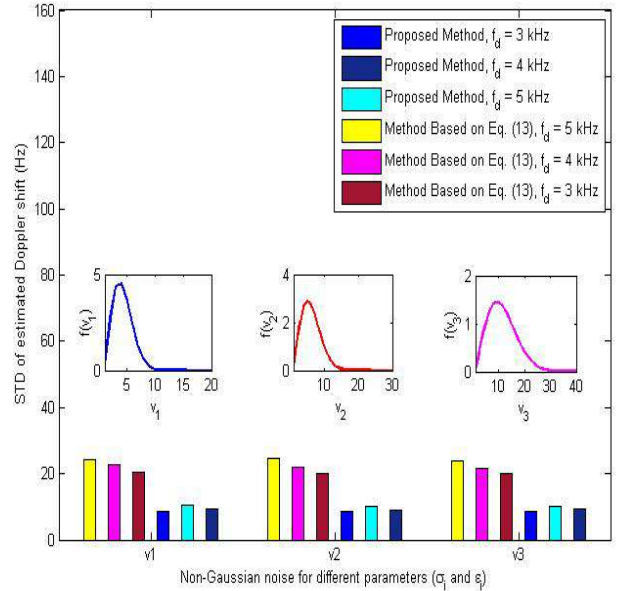
all kinds of the non-Gaussian noise that can be denoted by the GMM model. As we expected, the suggested algorithm can also be applied into those scenarios where the parameters of the non-Gaussian additive noise do not need to be considered in detail, and the better performance and relatively small Rice factor are required for the exploring communication system.

V. CONCLUSION

In this paper, we have investigated the problem on parameter estimation for the received space-based AIS signals from the satellite to the ship links. Moreover, a novel algorithm on the Doppler shift estimation has been proposed and studied for the received space-based AIS signals over the satellite-to-ship non-frequency selective Rician fading channels and non-Gaussian noise. The proposed method employs the second-order and fourth-order moments and their cooperations to eliminate some redundant signals and parameters. Further, useful expression for the Doppler shift estimation has been derived via reasonably mathematical calculating. The proposed method has been verified by computer simulations and the results illustrate that the suggested scheme is robust to the estimated frequency in its range with the Rice factor increments and all kinds of the non-Gaussian noise engendered by the GMM model. In addition, our approach can provide the good performance with the increases of the Rice factor, which also demonstrates the potential applications where there is a clear LoS path between the satellite and the ship or ocean user, without any obstacle between them, but it also permits some weakly indistinguishable NLoS paths coming from the scatterer if conditions on the estimation accuracy are rationally relaxed.

APPENDIX A
DERIVATION OF (13)

In this Appendix, we derive (13) as follows based on the identity mentioned in (13):

$$
\begin{aligned}
R_{zz}(m) &= E\{z^*(n) \cdot z(n+m)\} \\
&= E\Bigg\{ \bigg(\sqrt{\frac{K}{1+K}} \exp(-j2\pi\,\Delta f_d n - j\phi_0) \\
&\quad + \sqrt{\frac{1}{1+K}} h^*_{NLoS}(n) + v^*(n) \bigg) \\
&\quad \times \bigg(\sqrt{\frac{K}{1+K}} \exp\left(j2\pi\,\Delta f_d (n+m) + j\phi_0\right) \\
&\quad + \sqrt{\frac{1}{1+K}} h_{NLoS}(n+m) + v(n+m) \bigg) \Bigg\} \\
&= \frac{K}{1+K} \exp\left(j2\pi\,\Delta f_d m\right) + \frac{1}{1+K} J_0\left(2\pi f_d m\right) \\
&\quad + \sigma_v^2 \delta(m).
\end{aligned}
\tag{19}
$$

APPENDIX B
DERIVATION OF (15)

In this Appendix, we derive (15) as follows based on the identity mentioned in (13) and (15):

$$
R_{zzzz}(l, m, q) = E\{z^*(n) \cdot z(n+l) \cdot z(n+m) \cdot z^*(n+q)\}
$$

$$
= E\Bigg\{ \Bigg(\underbrace{\sqrt{\frac{K}{1+K}} \exp(-j2\pi\,\Delta f_d n - j\phi_0)}_{A1}
$$

$$
+ \underbrace{\sqrt{\frac{1}{1+K}} h^*_{NLoS}(n)}_{A2} + \underbrace{v^*(n)}_{A3} \Bigg)
$$

$$
\times \Bigg(\underbrace{\sqrt{\frac{K}{1+K}} \exp\left(j2\pi\,\Delta f_d (n+l) + j\phi_0\right)}_{B1}
$$

$$
+ \underbrace{\sqrt{\frac{1}{1+K}} h_{NLoS}(n+l)}_{B2} + \underbrace{v(n+l)}_{B3} \Bigg)
$$

$$
\times \Bigg(\underbrace{\sqrt{\frac{K}{1+K}} \exp\left(j2\pi\,\Delta f_d (n+m) + j\phi_0\right)}_{C1}
$$

$$
+ \underbrace{\sqrt{\frac{1}{1+K}} h_{NLoS}(n+m)}_{C2} + \underbrace{v(n+m)}_{C3} \Bigg)
$$

$$
\times \Bigg(\underbrace{\sqrt{\frac{K}{1+K}} \exp\left(-j2\pi\,\Delta f_d (n+q) - j\phi_0\right)}_{D1}
$$

$$
+ \underbrace{\sqrt{\frac{1}{1+K}} h^*_{NLoS}(n+q)}_{D2} + \underbrace{v^*(n+q)}_{D3} \Bigg) \Bigg\}
\tag{20}
$$

(20) is composed by the following equations we will calculate:

$$
E\{A1 \cdot B1 \cdot C1 \cdot D1\} = \left(\frac{K}{1+K}\right)^2 \exp\left(j2\pi\,\Delta f_d(l+m-q)\right),
\tag{21}
$$

$$
\begin{aligned}
E\{A1 \cdot B1 \cdot C1 \cdot D2\} &= E\{A1 \cdot B1 \cdot C1 \cdot D3\} \\
&= E\{A1 \cdot B1 \cdot C2 \cdot D1\} \\
&= E\{A1 \cdot B1 \cdot C2 \cdot D3\} \\
&= E\{A1 \cdot B1 \cdot C3 \cdot D1\} \\
&= E\{A1 \cdot B1 \cdot C3 \cdot D2\} \\
&= 0,
\end{aligned}
\tag{22}
$$

$$
\begin{aligned}
E\{A1 \cdot B1 \cdot C2 \cdot D2\} &= \frac{K}{(1+K)^2} \exp\left(j2\pi\,\Delta f_d l\right) \\
&\quad \cdot J_0\left(2\pi f_d(m-q)\right),
\end{aligned}
\tag{23}
$$

$$
E\{A1 \cdot B1 \cdot C3 \cdot D3\} = \frac{K}{1+K} \exp\left(j2\pi\,\Delta f_d l\right) \sigma_v^2 \delta(m-q),
\tag{24}
$$

$$
\begin{aligned}
E\{A1 \cdot B2 \cdot C1 \cdot D1\} &= E\{A1 \cdot B2 \cdot C1 \cdot D3\} \\
&= E\{A1 \cdot B2 \cdot C2 \cdot D1\} \\
&= E\{A1 \cdot B2 \cdot C2 \cdot D2\} \\
&= E\{A1 \cdot B2 \cdot C2 \cdot D3\} \\
&= E\{A1 \cdot B2 \cdot C3 \cdot D1\} \\
&= E\{A1 \cdot B2 \cdot C3 \cdot D2\} \\
&= E\{A1 \cdot B2 \cdot C3 \cdot D3\} \\
&= 0,
\end{aligned}
\tag{25}
$$

$$
\begin{aligned}
E\{A1 \cdot B2 \cdot C1 \cdot D2\} &= \frac{K}{(1+K)^2} \exp\left(j2\pi\,\Delta f_d m\right) \\
&\quad \cdot J_0\left(2\pi f_d(l-q)\right),
\end{aligned}
\tag{26}
$$

$$
\begin{aligned}
E\{A1 \cdot B3 \cdot C1 \cdot D1\} &= E\{A1 \cdot B3 \cdot C1 \cdot D2\} \\
&= E\{A1 \cdot B3 \cdot C2 \cdot D1\} \\
&= E\{A1 \cdot B3 \cdot C2 \cdot D2\} \\
&= E\{A1 \cdot B3 \cdot C2 \cdot D3\} \\
&= E\{A1 \cdot B3 \cdot C3 \cdot D1\} \\
&= E\{A1 \cdot B3 \cdot C3 \cdot D2\} \\
&= E\{A1 \cdot B3 \cdot C3 \cdot D3\} \\
&= 0,
\end{aligned}
\tag{27}
$$

$$
E\{A1 \cdot B3 \cdot C1 \cdot D3\} = \frac{K}{1+K} \exp\left(j2\pi\,\Delta f_d m\right) \sigma_v^2 \delta(l-q),
\tag{28}
$$

$$
\begin{aligned}
E\{A2 \cdot B1 \cdot C1 \cdot D1\} &= E\{A2 \cdot B1 \cdot C1 \cdot D2\}, \\
&= E\{A2 \cdot B1 \cdot C1 \cdot D3\} \\
&= E\{A2 \cdot B1 \cdot C2 \cdot D2\} \\
&= E\{A2 \cdot B1 \cdot C2 \cdot D3\} \\
&= E\{A2 \cdot B1 \cdot C3 \cdot D1\} \\
&= E\{A2 \cdot B1 \cdot C3 \cdot D2\} \\
&= E\{A2 \cdot B1 \cdot C3 \cdot D3\} \\
&= 0,
\end{aligned}
\tag{29}
$$

$$E\{A2 \cdot B1 \cdot C2 \cdot D1\} = \frac{K}{(1+K)^2} exp\big(j2\pi \Delta f_d(l-q)\big)$$
$$\cdot J_0(2\pi f_d m), \quad (30)$$

$$E\{A2 \cdot B2 \cdot C1 \cdot D1\} = \frac{K}{(1+K)^2} exp\big(j2\pi \Delta f_d(m-q)\big)$$
$$\cdot J_0(2\pi f_d l), \quad (31)$$

$$E\{A2 \cdot B2 \cdot C1 \cdot D2\} = E\{A2 \cdot B2 \cdot C1 \cdot D3\}$$
$$= E\{A2 \cdot B2 \cdot C2 \cdot D1\}$$
$$= E\{A2 \cdot B2 \cdot C2 \cdot D3\}$$
$$= E\{A2 \cdot B2 \cdot C3 \cdot D1\}$$
$$= E\{A2 \cdot B2 \cdot C3 \cdot D2\}$$
$$= 0, \quad (32)$$

$$E\{A2 \cdot B2 \cdot C2 \cdot D2\} = \frac{1}{(1+K)^2}\Big\{J_0\left(2\pi f_d l\right)$$
$$\cdot J_0\big(2\pi f_d(m-q)\big)$$
$$+ J_0\left(2\pi f_d m\right) J_0\big(2\pi f_d(l-q)\big)\Big\}, \quad (33)$$

$$E\{A2 \cdot B2 \cdot C3 \cdot D3\} = \frac{1}{1+K}J_0\left(2\pi f_d l\right)\sigma_v^2\delta(m-q), \quad (34)$$

$$E\{A2 \cdot B3 \cdot C1 \cdot D1\} = E\{A2 \cdot B3 \cdot C1 \cdot D2\}$$
$$= E\{A2 \cdot B3 \cdot C1 \cdot D3\}$$
$$= E\{A2 \cdot B3 \cdot C2 \cdot D1\}$$
$$= E\{A2 \cdot B3 \cdot C2 \cdot D2\}$$
$$= E\{A2 \cdot B3 \cdot C3 \cdot D1\}$$
$$= E\{A2 \cdot B3 \cdot C3 \cdot D2\}$$
$$= E\{A2 \cdot B3 \cdot C3 \cdot D3\}$$
$$= 0, \quad (35)$$

$$E\{A2 \cdot B3 \cdot C2 \cdot D3\} = \frac{1}{1+K}J_0\left(2\pi f_d m\right)\sigma_v^2\delta(l-q), \quad (36)$$

$$E\{A3 \cdot B1 \cdot C1 \cdot D1\} = E\{A3 \cdot B1 \cdot C1 \cdot D2\}$$
$$= E\{A3 \cdot B1 \cdot C1 \cdot D3\}$$
$$= E\{A3 \cdot B1 \cdot C2 \cdot D1\}$$
$$= E\{A3 \cdot B1 \cdot C2 \cdot D2\}$$
$$= E\{A3 \cdot B1 \cdot C2 \cdot D3\}$$
$$= E\{A3 \cdot B1 \cdot C3 \cdot D2\}$$
$$= E\{A3 \cdot B1 \cdot C3 \cdot D3\}$$
$$= 0, \quad (37)$$

$$E\{A3 \cdot B1 \cdot C3 \cdot D1\} = \frac{K}{1+K}exp\big(j2\pi \Delta f_d(l-q)\big)\sigma_v^2\delta(m), \quad (38)$$

$$E\{A3 \cdot B2 \cdot C1 \cdot D1\} = E\{A3 \cdot B2 \cdot C1 \cdot D2\}$$
$$= E\{A3 \cdot B2 \cdot C1 \cdot D3\}$$
$$= E\{A3 \cdot B2 \cdot C2 \cdot D1\}$$
$$= E\{A3 \cdot B2 \cdot C2 \cdot D2\}$$
$$= E\{A3 \cdot B2 \cdot C2 \cdot D3\}$$
$$= E\{A3 \cdot B2 \cdot C3 \cdot D1\}$$
$$= E\{A3 \cdot B2 \cdot C3 \cdot D3\}$$
$$= 0, \quad (39)$$

$$E\{A3 \cdot B2 \cdot C3 \cdot D2\} = \frac{1}{1+K}J_0\big(2\pi f_d(l-q)\big)\sigma_v^2\delta(m), \quad (40)$$

$$E\{A3 \cdot B3 \cdot C1 \cdot D1\} = \frac{K}{1+K}exp\big(j2\pi \Delta f_d(m-q)\big)\sigma_v^2\delta(l), \quad (41)$$

$$E\{A3 \cdot B3 \cdot C1 \cdot D2\} = E\{A3 \cdot B3 \cdot C1 \cdot D3\}$$
$$= E\{A3 \cdot B3 \cdot C2 \cdot D1\}$$
$$= E\{A3 \cdot B3 \cdot C2 \cdot D3\}$$
$$= E\{A3 \cdot B3 \cdot C3 \cdot D1\}$$
$$= E\{A3 \cdot B3 \cdot C3 \cdot D2\}$$
$$= 0, \quad (42)$$

$$E\{A3 \cdot B3 \cdot C2 \cdot D2\} = \frac{1}{1+K}J_0\big(2\pi f_d(m-q)\big)\sigma_v^2\delta(l), \quad (43)$$

$$E\{A3 \cdot B3 \cdot C3 \cdot D3\} = \sigma_v^4\delta(l)\delta(m-q) + \sigma_v^4\delta(m)\delta(l-q). \quad (44)$$

Based on the above equations from (21) to (44), we then add them together, and conclude the derivation.

REFERENCES
[1] J. Wang, Y. Cui, S. Ma, X. Meng, L. Liu, and J. Teng, "A non-isotropic simulation model for ship-to-ship fading channels," in *Proc. 6th Int. Conf. Wireless, Mobile Multi-Media*, 2015, pp. 115–119.

[2] J. Wang, Y. Cui, S. Ma, X. Meng, and Z. Liu, "A scheme designed for cognitive automatic identification system," China Patent 201 510 995 727 .2, Dec. 29, 2015.

[3] J. Wang, Y. Cui, S. Ma, Z. Liu, L. Liu, and J. Teng, "On the spectrum sensing for cognitive automatic identification system," in *Proc. IEEE 13th Int. Conf. Signal Process. (ICSP)*, Nov. 2016, pp. 1313–1317.

[4] J. Wang, Y. Cui, S. Ma, L. Liu, and J. Teng, "PAPR reduction for cognitive AIS using transforming sequence of Frank-Heimiller and artificial bee colony algorithm," in *Proc. Int. Conf. Commun., Signal Process., Syst.*, Oct. 2016, pp. 97–105.

[5] T. Pratt, C. Bostian, and J. Allnutt, *Satellite Communications*. 2nd ed., New York, NY, USA: Wiley, 2003.

[6] G. Maral, M. Bousquet, and Z. Sun, *Satellite Communications Systems: Systems, Techniques and Technology*, 5th ed. New York, NY, USA: Wiley, 2009.

[7] K. Y. Jo, *Satellite Communications Network Design and Analysis*. Norwood, MA, USA: Artech House, 2011.

[8] M. Picard, M. R. Oularbi, G. Flandin, and S. Houcke, "An adaptive multi-user multi-antenna receiver for satellite-based AIS detection," in *Proc. 6th Adv. Satell. Multimedia Syst. Conf. (ASMS)*, Sep. 2012, pp. 273–280.

[9] Y. Ma and S. Ma, "An improved fastica algorithm for signal separation of satellite-based AIS," in *Proc. Int. Conf. Inf. Commun. Technol.*, May 2014, pp. 1–4.

[10] S. Ma and Y. Ma, "Improvement of complex fast independent component analysis algorithm for satellite-based AIS," *Telecommun. Eng.*, vol. 55, no. 6, pp. 639–644, Jun. 2015.

[11] J. Hao, S. Ma, J. Wang, and X. Meng, "Multiple-Symbol combined differential detection for satellite-based AIS signals," *J. Adv. Signal Process.*, vol. 64, pp. 1–12, Dec. 2015.

[12] P. Burzigotti, A. Ginesi, and G. Colavolpe, "Advanced receiver design for satellite-based AIS signal detection," in *Proc. 5th Adv. Satell. Multimedia Syst. Conf.*, Sep. 2010, pp. 1–8.

[13] S. Ma, C. Liu, and J. Wang, "An accurate frequency offset estimator in the intermediate frequency for the satellite-based AIS signals," in *Proc. IEEE Int. Conf. Online Anal. Comput. Sci. (ICOACS)*, May 2016, pp. 100–104.

[14] X. Meng, S. Ma, C. Liu, and J. Teng, "Frequency offset estimation in the intermediate frequency for satellite-based AIS signals," *Optoelectron. Lett.*, vol. 14, no. 4, pp. 301–305, Jul. 2018.

[15] X. Meng, C. Liu, J. Teng, and S. Ma, "Frequency offset estimation of satellite-based AIS signals based on interpolated FFT," *Wireless Pers. Commun.*, vol. 99, no. 1, pp. 35–45, Mar. 2018.

[16] J. Hagenauer, F. Dolainsky, E. Lutz, W. Papke, and R. Schweikert, "The maritime satellite communication channel–channel model, performance of modulation and coding," *IEEE J. Sel. Areas Commun.*, vol. 5, no. 4, pp. 701–713, May 1987.

[17] V. I. Lutsenko, I. V. Lutsenko, and I. V. Popov, "Adaptive and nonparametric methods of signal detection against the background of non-Gaussian clutter from underlying surface," in *Proc. Eur. Radar Conf.*, Oct. 2010, pp. 392–395.

[18] G. P. Kulemin and V. I. Lutsenko, "Microwave scattering from the sea surface," *Telecommun. Radio Eng.*, vol. 51, nos. 2–3, pp. 25–46, May 1997.

[19] V. I. Lutsenko, "Imitation model of the signal scattered back from sea surface," *Program Mod. Radio Electron.*, vol. 4, pp. 59–73, Aug. 2008.

[20] J. Wang, X. Ma, J. Teng, and Y. Cui, "Efficient and accurate simulator for Rayleigh and Rician fading," *Trans. Tianjin Univ.*, vol. 18, no. 4, pp. 243–247, Aug. 2012.

[21] J. Wang, Y. Cui, H. Sun, L. Liu, and S. Ma, "Full-duplex cognitive underwater acoustic communications: Concept and challenges," in *Proc. 14th IEEE Int. Conf. Signal Process. (ICSP)*, Aug. 2018, pp. 698–701.

JUNFENG WANG received the Ph.D. degree in information and communication engineering from the School of Electronic Information Engineering, Tianjin University, China, in 2012. At the same year, he joined the Tianjin University of Technology, where he is currently an Assistant Professor with the Department of Information and Communication Engineering, School of Electrical and Electronic Engineering. He is also a Research Scholar with the Missouri University of Science and Technology, USA.

His current research interests include wireless communications and signal processing.

He was the recipient of the "2008 Excellent Master Thesis Award" and the "2012 Outstanding Graduate Research Achievement Award." He received the Best Paper Award at the 5th International Conference on Communications, Signal Processing, and Systems. He is/has served as a Technical Program Committee Member and Session Chair for several IEEE/IET conferences, and as a Reviewer of numerous IEEE/IET journals and conferences.

YUE CUI received the Ph.D. degree in circuit and system from the School of Electronic Information Engineering, Tianjin University, China, in 2012. At the same year, she joined the Tianjin Normal University, where she is currently an Assistant Professor with the Department of Information Engineering, School of Computer and Information Engineering. She is also a Research Scholar with the Missouri University of Science and Technology, USA.

Her current research interests include array signal processing and unstationary signal processing.

She was the recipient of the Best Paper Award, in 2016, and Faculty Excellence Award, in 2015. She is also a Reviewer for many IEEE/IET top journals and conferences.

HAIXIN SUN (M'13) received the B.S. and M.S. degrees in electronic engineering from Shandong University of Science and Technology, Shandong, China, in 1999 and 2003, respectively, and the Ph.D. degree in communication engineering from the Institute of Acoustic, Chinese Academy of Science, Shanghai, China, in 2006. He visited the Department of Electrical and Computer Engineering, University of Connecticut, Storrs, USA, from March 2012 to April 2013. He is currently an Associate Professor and Doctoral Advisor with the School of Information Science and Engineering, Xiamen University.

His current research interests include underwater acoustic communication, network, and signal processing.

He is the member of the IEICE. He was awarded Huawei Fellowship of Xiamen University, in 2010, Faculty of Engineering Excellence Award of Xiamen University, and Prize of Chinese Army Scientific and Technological, in 2017. He has served as a Reviewer for journals and conferences.

JIANGHUI LI received the B.S. degree in communications engineering from Huazhong University of Science and Technology, Wuhan, China, in 2011, the M.S. degree in communications engineering, and the Ph.D. degree with receiving the K. M. Stott Prize for excellent research in electronics engineering from the University of York, U.K., in 2013 and 2017, respectively. He has been the first researcher receiving the IEEE OES scholarship in U.K. From 2011 to 2012, he served as a Research Assistant with the Chinese Academy of Sciences, Beijing, China. Since 2017, he has been a Research Fellow with the University of Southampton, U.K.

His current research interests include adaptive signal processing, wireless communications, underwater acoustics, and ocean engineering.

MINGZHANG ZHOU received the B.S. degree in communication engineering from the School of Information Science and Technology, Xiamen University, Xiamen, China, in 2017, where he is currently pursuing the Ph.D. degree.

His research interests include channel coding and parameter estimation for wireless communication systems, signal detection for OFDM communication systems, and deep learning and its application in underwater acoustic communications and signal processing.

ZEYAD A. H. QASEM received the B.S. degree in electronics engineering and the M.S. degree in digital systems of telecommunications from the University of Sidi Bel Abbes, Algeria, in 2011 and 2013, respectively. From 2014 to 2017, he worked for Huawei Company as an Engineer for the core networks. He is currently pursuing the Ph.D. degree with the School of Information Science and Technology, Xiamen University, Xiamen, China.

His research interests include equalization, frequency and channel estimation, and signal detection in OFDM, MIMO, and QoS enhancement in ad hoc sensor networks and compress sensing.

HAMADA ESMAIEL (M'18) received the B.E. degree (with first-class Hons.) in electrical engineering and the M.S. degree in wireless communications from the South Valley University, Egypt, in 2005 and 2010, respectively, and the Ph.D. degree in communication engineering from the University of Tasmania, Australia, in 2015. In 2011, he was a Research Assistant with the Wireless Communication Laboratory, Wonkwang University, Iksan, South Korea. Since 2015, he has been an Assistant Professor with Aswan University, Egypt. Also, he has been with the University of Ryukyus, Nishihara, Okinawa, Japan, as a Visiting Researcher, since 2018.

His research interests include 5G cellular networks, Li-Fi technology, millimetre-wave transmissions, underwater communication, and MIMO systems.

He is the General Co-Chair of the IEEE ISWC'18. He is a Technical Committee Member of many international conferences and a Reviewer of many international conferences, journals, and transactions.

LANJUN LIU received the B.S. degree in automation and the M.S. degree in signal and information processing from Ocean University of China, Qingdao, China, in 2002 and 2005, respectively, and the Ph.D. degree in computer application technology from the University of Science and Technology Beijing, Beijing, China, in 2009. At the same year, he joined the Ocean University of China, where he is currently an Associate Professor and Master Advisor.

His research interests include underwater acoustic communication and networks, submarine observation, and detection technology and equipment.

● ● ●